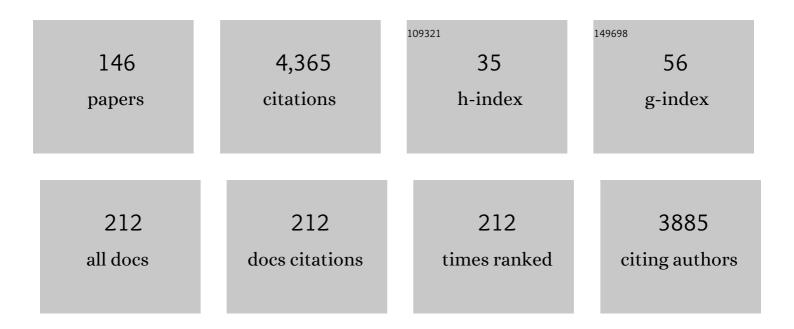
Stefan A Buehler

List of Publications by Year in descending order

Source: https://exaly.com/author-pdf/664575/publications.pdf Version: 2024-02-01



#	Article	IF	CITATIONS
1	ARTS, the atmospheric radiative transfer simulator, version 2. Journal of Quantitative Spectroscopy and Radiative Transfer, 2011, 112, 1551-1558.	2.3	222
2	ARTS, the atmospheric radiative transfer simulator. Journal of Quantitative Spectroscopy and Radiative Transfer, 2005, 91, 65-93.	2.3	218
3	State of the Climate in 2017. Bulletin of the American Meteorological Society, 2018, 99, Si-S310.	3.3	160
4	Qpack, a general tool for instrument simulation and retrieval work. Journal of Quantitative Spectroscopy and Radiative Transfer, 2005, 91, 47-64.	2.3	142
5	State of the Climate in 2016. Bulletin of the American Meteorological Society, 2017, 98, Si-S280.	3.3	132
6	ARTS, the Atmospheric Radiative Transfer Simulator – version 2.2, the planetary toolbox edition. Geoscientific Model Development, 2018, 11, 1537-1556.	3.6	102
7	A concept for a satellite mission to measure cloud ice water path, ice particle size, and cloud altitude. Quarterly Journal of the Royal Meteorological Society, 2007, 133, 109-128.	2.7	100
8	The Added Value of Large-eddy and Storm-resolving Models for Simulating Clouds and Precipitation. Journal of the Meteorological Society of Japan, 2020, 98, 395-435.	1.8	93
9	Simulated Tropical Precipitation Assessed across Three Major Phases of the Coupled Model Intercomparison Project (CMIP). Monthly Weather Review, 2020, 148, 3653-3680.	1.4	92
10	Assessing observed and modelled spatial distributions of ice water path using satellite data. Atmospheric Chemistry and Physics, 2011, 11, 375-391.	4.9	90
11	EUREC ⁴ A. Earth System Science Data, 2021, 13, 4067-4119.	9.9	88
12	Representative wavelengths absorption parameterization applied to satellite channels and spectral bands. Journal of Quantitative Spectroscopy and Radiative Transfer, 2014, 148, 99-115.	2.3	82
13	A general database of hydrometeor single scattering properties at microwave and sub-millimetre wavelengths. Earth System Science Data, 2018, 10, 1301-1326.	9.9	74
14	Intercomparison of general purpose clear sky atmospheric radiative transfer models for the millimeter/submillimeter spectral range. Radio Science, 2005, 40, n/a-n/a.	1.6	71
15	A polarized discrete ordinate scattering model for simulations of limb and nadir long-wave measurements in 1-D/3-D spherical atmospheres. Journal of Geophysical Research, 2004, 109, .	3.3	68
16	A simple method to relate microwave radiances to upper tropospheric humidity. Journal of Geophysical Research, 2005, 110, .	3.3	66
17	Global Climate. Bulletin of the American Meteorological Society, 2020, 101, S9-S128.	3.3	61
18	Water vapor continuum: absorption measurements at and model calculations. Journal of Quantitative Spectroscopy and Radiative Transfer, 2002, 74, 545-562.	2.3	58

#	Article	IF	CITATIONS
19	Radiative flux and forcing parameterization error in aerosolâ€free clear skies. Geophysical Research Letters, 2015, 42, 5485-5492.	4.0	57
20	A multi-instrument comparison of integrated water vapour measurements at a high latitude site. Atmospheric Chemistry and Physics, 2012, 12, 10925-10943.	4.9	55
21	Clear-sky biases in satellite infrared estimates of upper tropospheric humidity and its trends. Journal of Geophysical Research, 2011, 116, .	3.3	53
22	Performance simulations for a submillimetre-wave satellite instrument to measure cloud ice. Quarterly Journal of the Royal Meteorological Society, 2007, 133, 129-149.	2.7	52
23	Using CHAMP radio occultation data to determine the top altitude of the Planetary Boundary Layer. Geophysical Research Letters, 2005, 32, .	4.0	51
24	Observing ice clouds in the submillimeter spectral range: the CloudIce mission proposal for ESA's Earth Explorer 8. Atmospheric Measurement Techniques, 2012, 5, 1529-1549.	3.1	51
25	An upper tropospheric humidity data set from operational satellite microwave data. Journal of Geophysical Research, 2008, 113, .	3.3	50
26	A cloud filtering method for microwave upper tropospheric humidity measurements. Atmospheric Chemistry and Physics, 2007, 7, 5531-5542.	4.9	44
27	The impact of ozone lines on AMSU-B radiances. Geophysical Research Letters, 2004, 31, n/a-n/a.	4.0	43
28	Interannual to Diurnal Variations in Tropical and Subtropical Deep Convective Clouds and Convective Overshooting from Seven Years of AMSU-B Measurements. Journal of Climate, 2008, 21, 4168-4189.	3.2	43
29	Comparison of microwave satellite humidity data and radiosonde profiles: A case study. Journal of Geophysical Research, 2004, 109, n/a-n/a.	3.3	42
30	Scattering database in the millimeter and submillimeter wave range of 100–1000 GHz for nonspherical ice particles. Journal of Geophysical Research, 2009, 114, .	3.3	41
31	A review of sources of systematic errors and uncertainties in observations and simulations at 183†GHz. Atmospheric Measurement Techniques, 2016, 9, 2207-2221.	3.1	41
32	FORUM: Unique Far-Infrared Satellite Observations to Better Understand How Earth Radiates Energy to Space. Bulletin of the American Meteorological Society, 2020, 101, E2030-E2046.	3.3	40
33	Instrumental and spectral parameters: their effect on and measurement by microwave limb sounding of the atmosphere. Journal of Quantitative Spectroscopy and Radiative Transfer, 2000, 64, 421-437.	2.3	39
34	Understanding intersatellite biases of microwave humidity sounders using global simultaneous nadir overpasses. Journal of Geophysical Research, 2012, 117, .	3.3	39
35	Middle-atmospheric zonal and meridional wind profiles from polar, tropical and midlatitudes with the ground-based microwave Doppler wind radiometer WIRA. Atmospheric Measurement Techniques, 2014, 7, 4491-4505.	3.1	39
36	OceanRAIN, a new in-situ shipboard global ocean surface-reference dataset of all water cycle components. Scientific Data, 2018, 5, 180122.	5.3	39

#	Article	IF	CITATIONS
37	3-D polarised simulations of space-borne passive mm/sub-mm midlatitude cirrus observations: a case study. Atmospheric Chemistry and Physics, 2007, 7, 4149-4158.	4.9	36
38	On the microwave optical properties of randomly oriented ice hydrometeors. Atmospheric Measurement Techniques, 2015, 8, 1913-1933.	3.1	36
39	Comparison of microwave satellite humidity data and radiosonde profiles: A survey of European stations. Atmospheric Chemistry and Physics, 2005, 5, 1843-1853.	4.9	35
40	Molecular Line Parameters for the "MASTER―(Millimeter Wave Acquisitions for) Tj ETQq0 0 0 rgBT /Overloc 161-205.	k 10 Tf 50 3.2	627 Td (Stra 35
41	Scan asymmetries in AMSU-B data. Geophysical Research Letters, 2005, 32, .	4.0	35
42	NO ₂ Profile retrieval using airborne multi axis UV-visible skylight absorption measurements over central Europe. Atmospheric Chemistry and Physics, 2006, 6, 3049-3058.	4.9	35
43	Towards an operational Ice Cloud Imager (ICI) retrieval product. Atmospheric Measurement Techniques, 2020, 13, 53-71.	3.1	35
44	Retrieval of profile information from airborne multiaxis UV-visible skylight absorption measurements. Applied Optics, 2004, 43, 4415.	2.1	33
45	Non-Gaussian Bayesian retrieval of tropical upper tropospheric cloud ice and water vapour from Odin-SMR measurements. Atmospheric Measurement Techniques, 2009, 2, 621-637.	3.1	33
46	Recent developments in the line-by-line modeling of outgoing longwave radiation. Journal of Quantitative Spectroscopy and Radiative Transfer, 2006, 98, 446-457.	2.3	32
47	SPARE″CE: Synergistic ice water path from passive operational sensors. Journal of Geophysical Research D: Atmospheres, 2014, 119, 1504-1523.	3.3	32
48	The potential of polarization measurements from space at mm and sub-mm wavelengths for determining cirrus cloud parameters. Atmospheric Chemistry and Physics, 2003, 3, 39-48.	4.9	31
49	Absorption lookup tables in the radiative transfer model ARTS. Journal of Quantitative Spectroscopy and Radiative Transfer, 2011, 112, 1559-1567.	2.3	31
50	Retrieval of an ice water path over the ocean from ISMAR and MARSS millimeter and submillimeter brightness temperatures. Atmospheric Measurement Techniques, 2018, 11, 611-632.	3.1	31
51	A sensitivity study on spectroscopic parameter accuracies for a mm/sub-mm limb sounder instrument. Journal of Molecular Spectroscopy, 2005, 229, 266-275.	1.2	30
52	Collocating satellite-based radar and radiometer measurements – methodology and usage examples. Atmospheric Measurement Techniques, 2010, 3, 693-708.	3.1	30
53	A treatment of the Zeeman effect using Stokes formalism and its implementation in the Atmospheric Radiative Transfer Simulator (ARTS). Journal of Quantitative Spectroscopy and Radiative Transfer, 2014, 133, 445-453.	2.3	30
54	Radiative transfer calculations for a passive microwave satellite sensor: Comparing a fast model and a line-by-line model. Journal of Geophysical Research, 2006, 111, .	3.3	28

#	Article	IF	CITATIONS
55	Validation of water vapour profiles (version 13) retrieved by the IMK/IAA scientific retrieval processor based on full resolution spectra measured by MIPAS on board Envisat. Atmospheric Measurement Techniques, 2009, 2, 379-399.	3.1	28
56	Monitoring scan asymmetry of microwave humidity sounding channels using simultaneous all angle collocations (SAACs). Journal of Geophysical Research D: Atmospheres, 2013, 118, 1536-1545.	3.3	28
57	How Robust Is the Weakening of the Pacific Walker Circulation in CMIP5 Idealized Transient Climate Simulations?. Journal of Climate, 2018, 31, 81-97.	3.2	28
58	Re-Examining the First Climate Models: Climate Sensitivity of a Modern Radiative–Convective Equilibrium Model. Journal of Climate, 2019, 32, 8111-8125.	3.2	27
59	Efficient radiative transfer simulations for a broadband infrared radiometer—Combining a weighted mean of representative frequencies approach with frequency selection by simulated annealing. Journal of Quantitative Spectroscopy and Radiative Transfer, 2010, 111, 602-615.	2.3	26
60	On the Importance of Vaisala RS92 Radiosonde Humidity Corrections for a Better Agreement between Measured and Modeled Satellite Radiances. Journal of Atmospheric and Oceanic Technology, 2012, 29, 248-259.	1.3	26
61	The Dependence of Shallow Cumulus Macrophysical Properties on Largeâ€6cale Meteorology as Observed in ASTER Imagery. Journal of Geophysical Research D: Atmospheres, 2019, 124, 11477-11505.	3.3	25
62	Towards more realistic hypotheses for the information content analysis of cloudy/precipitating situations – Application to a hyperspectral instrument in the microwave. Quarterly Journal of the Royal Meteorological Society, 2019, 145, 1-14.	2.7	23
63	Efficient forward modelling by matrix representation of sensor responses. International Journal of Remote Sensing, 2006, 27, 1793-1808.	2.9	22
64	Emerging Technologies and Synergies for Airborne and Space-Based Measurements of Water Vapor Profiles. Surveys in Geophysics, 2017, 38, 1445-1482.	4.6	22
65	Intercomparison of three microwave/infrared high resolution line-by-line radiative transfer codes. Journal of Quantitative Spectroscopy and Radiative Transfer, 2018, 211, 64-77.	2.3	22
66	Prediction of cloud ice signatures in submillimetre emission spectra by means of ground-based radar and in situ microphysical data. Quarterly Journal of the Royal Meteorological Society, 2007, 133, 151-162.	2.7	21
67	A strong ice cloud event as seen by a microwave satellite sensor: Simulations and observations. Journal of Quantitative Spectroscopy and Radiative Transfer, 2008, 109, 1705-1718.	2.3	21
68	Comparing upper tropospheric humidity data from microwave satellite instruments and tropical radiosondes. Journal of Geophysical Research, 2010, 115, .	3.3	21
69	Benchmark Calculations of Radiative Forcing by Greenhouse Gases. Journal of Geophysical Research D: Atmospheres, 2020, 125, e2020JD033483.	3.3	21
70	Robust and Nonrobust Impacts of Atmospheric Cloudâ€Radiative Interactions on the Tropical Circulation and Its Response to Surface Warming. Geophysical Research Letters, 2018, 45, 8577-8585.	4.0	20
71	Microwave and submillimeter wave scattering of oriented ice particles. Atmospheric Measurement Techniques, 2020, 13, 2309-2333.	3.1	20
72	Assessment of intercalibration methods for satellite microwave humidity sounders. Journal of Geophysical Research D: Atmospheres, 2013, 118, 4906-4918.	3.3	19

#	Article	IF	CITATIONS
73	Systematic and random errors between collocated satellite ice water path observations. Journal of Geophysical Research D: Atmospheres, 2013, 118, 2629-2642.	3.3	19
74	A 1D RCE Study of Factors Affecting the Tropical Tropopause Layer and Surface Climate. Journal of Climate, 2019, 32, 6769-6782.	3.2	19
75	Zeeman effect in atmospheric O ₂ measured by ground-based microwave radiometry. Atmospheric Measurement Techniques, 2015, 8, 1863-1874.	3.1	18
76	Noise performance of microwave humidity sounders over their lifetime. Atmospheric Measurement Techniques, 2017, 10, 4927-4945.	3.1	18
77	The Representation of Tropospheric Water Vapor Over Low-Latitude Oceans in (Re-)analysis: Errors, Impacts, and the Ability to Exploit Current and Prospective Observations. Surveys in Geophysics, 2017, 38, 1399-1423.	4.6	17
78	A Hotelling transformation approach for rapid inversion of atmospheric spectra. Journal of Quantitative Spectroscopy and Radiative Transfer, 2002, 73, 529-543.	2.3	16
79	Correcting diurnal cycle aliasing in satellite microwave humidity sounder measurements. Journal of Geophysical Research D: Atmospheres, 2013, 118, 101-113.	3.3	16
80	Geometric estimation of volcanic eruption column height from GOES-R near-limb imagery – Part 2: Case studies. Atmospheric Chemistry and Physics, 2021, 21, 12207-12226.	4.9	16
81	The Moon as a photometric calibration standard for microwave sensors. Atmospheric Measurement Techniques, 2016, 9, 3467-3475.	3.1	16
82	Variability of Indian summer monsoon in a new upper tropospheric humidity data set. Geophysical Research Letters, 2010, 37, .	4.0	15
83	Partition function data and impact on retrieval quality for an mm/sub-mm limb sounder. Journal of Quantitative Spectroscopy and Radiative Transfer, 2005, 90, 217-238.	2.3	14
84	Evaluating the Diurnal Cycle of Upper Tropospheric Humidity in Two Different Climate Models Using Satellite Observations. Remote Sensing, 2016, 8, 325.	4.0	14
85	Information content on hydrometeors from millimeter and sub-millimeter wavelengths. Tellus, Series A: Dynamic Meteorology and Oceanography, 2022, 69, 1271562.	1.7	14
86	An Uncertainty Quantified Fundamental Climate Data Record for Microwave Humidity Sounders. Remote Sensing, 2019, 11, 548.	4.0	14
87	On cloud ice induced absorption and polarisation effects in microwave limb sounding. Atmospheric Measurement Techniques, 2011, 4, 1305-1318.	3.1	13
88	Evolution of an Atmospheric Kármán Vortex Street From Highâ€Resolution Satellite Winds: Guadalupe Island Case Study. Journal of Geophysical Research D: Atmospheres, 2020, 125, e2019JD032121.	3.3	13
89	A Cautionary Note on the Use of Gaussian Statistics in Satellite-Based UTH Climatologies. IEEE Geoscience and Remote Sensing Letters, 2006, 3, 130-134.	3.1	12
90	Comparison of AIRS and AMSUâ€B monthly mean estimates of upper tropospheric humidity. Geophysical Research Letters, 2009, 36, .	4.0	12

#	Article	IF	CITATIONS
91	Performance of Radiative Transfer Models in the Microwave Region. Journal of Geophysical Research D: Atmospheres, 2020, 125, e2019JD031831.	3.3	12
92	The impact of temperature errors on perceived humidity supersaturation. Geophysical Research Letters, 2003, 30, .	4.0	11
93	The effect of cirrus clouds on microwave limb radiances. Atmospheric Research, 2004, 72, 383-401.	4.1	11
94	The natural greenhouse effect of atmospheric oxygen (O ₂) and nitrogen (N ₂). Geophysical Research Letters, 2012, 39, .	4.0	11
95	Is There Really a Closure Gap Between 183.31-GHz Satellite Passive Microwave and <italic>In Situ</italic> Radiosonde Water Vapor Measurements?. IEEE Transactions on Geoscience and Remote Sensing, 2018, 56, 2904-2910.	6.3	11
96	Geometric estimation of volcanic eruption column height from GOES-R near-limb imagery – Part 1: Methodology. Atmospheric Chemistry and Physics, 2021, 21, 12189-12206.	4.9	11
97	Understanding the variability of clear-sky outgoing long-wave radiation based on ship-based temperature and water vapour measurements. Quarterly Journal of the Royal Meteorological Society, 2006, 132, 2675-2691.	2.7	10
98	The Fast Response of the Tropical Circulation to CO ₂ Forcing. Journal of Climate, 2018, 31, 9903-9920.	3.2	10
99	Evaluating Instrumental Inhomogeneities in Global Radiosonde Upper Tropospheric Humidity Data Using Microwave Satellite Data. IEEE Transactions on Geoscience and Remote Sensing, 2013, 51, 3615-3624.	6.3	9
100	Simulation of Ship-Track versus Satellite-Sensor Differences in Oceanic Precipitation Using an Island-Based Radar. Remote Sensing, 2017, 9, 593.	4.0	9
101	Towards an alongâ€ŧrack validation of HOAPS precipitation using OceanRAIN optical disdrometer data over the Atlantic Ocean. Quarterly Journal of the Royal Meteorological Society, 2018, 144, 235-254.	2.7	9
102	A simple new radiative transfer model for simulating the effect of cirrus clouds in the microwave spectral region. Journal of Quantitative Spectroscopy and Radiative Transfer, 2002, 75, 611-624.	2.3	8
103	Understanding the polarization signal of spherical particles for microwave limb radiances. Journal of Quantitative Spectroscopy and Radiative Transfer, 2006, 101, 179-190.	2.3	8
104	A method for remote sensing of weak planetary magnetic fields: Simulated application to Mars. Geophysical Research Letters, 2013, 40, 5014-5018.	4.0	8
105	Seasonal variation of coherence in SAR interferograms in Kiruna, Northern Sweden. International Journal of Remote Sensing, 2016, 37, 370-387.	2.9	8
106	Disk-Integrated Lunar Brightness Temperatures between 89 and 190 GHz. Advances in Astronomy, 2019, 2019, 1-8.	1.1	8
107	Tropical Freeâ€Tropospheric Humidity Differences and Their Effect on the Clearâ€Sky Radiation Budget in Global Stormâ€Resolving Models. Journal of Advances in Modeling Earth Systems, 2021, 13, .	3.8	8
108	Synergistic radar and radiometer retrievals of ice hydrometeors. Atmospheric Measurement Techniques, 2020, 13, 4219-4245.	3.1	8

#	Article	IF	CITATIONS
109	Temperatureâ€Dependence of the Clearâ€Sky Feedback in Radiativeâ€Convective Equilibrium. Geophysical Research Letters, 2021, 48, .	4.0	8
110	A practical demonstration on AMSU retrieval precision for upper tropospheric humidity by a non-linear multi-channel regression method. Atmospheric Chemistry and Physics, 2005, 5, 451-459.	4.9	7
111	Expected performance of the Superconducting Submillimeter-Wave Limb Emission Sounder compared with aircraft data. Radio Science, 2005, 40, n/a-n/a.	1.6	7
112	Observing cosmic microwave background polarization through ice. Monthly Notices of the Royal Astronomical Society, 2007, 376, 645-650.	4.4	7
113	Ensemble Optimization Retrieval Algorithm of Hydrometeor Profiles for the Ice Cloud Imager Submillimeterâ€Wave Radiometer. Journal of Geophysical Research D: Atmospheres, 2018, 123, 4594-4612.	3.3	7
114	Evaluation of the EUMETSAT Global AVHRR Wind Product. Journal of Applied Meteorology and Climatology, 2017, 56, 2353-2376.	1.5	6
115	All-sky information content analysis for novel passive microwave instruments in the range from 23.8 to 874.4 GHz. Atmospheric Measurement Techniques, 2018, 11, 4217-4237.	3.1	6
116	The sensitivity of oceanic precipitation to sea surface temperature. Atmospheric Chemistry and Physics, 2019, 19, 9241-9252.	4.9	6
117	Trends in Upper-Tropospheric Humidity: Expansion of the Subtropical Dry Zones?. Journal of Climate, 2020, 33, 2149-2161.	3.2	6
118	Temperature profile retrieval from surface to mesopause by combining GNSS Radio Occultation and Passive Microwave Limb Sounder Data. Geophysical Research Letters, 2001, 28, 775-778.	4.0	5
119	Interference from terrestrial sources and its impact on the GRAS GPS radio occultation receiver. Radio Science, 2014, 49, 1-6.	1.6	5
120	THz spectroscopy of the atmosphere for climatology and meteorology applications. , 2017, , .		5
121	The Moon at thermal infrared wavelengths: a benchmark for asteroid thermal models. Astronomy and Astrophysics, 2021, 650, A38.	5.1	5
122	Synergistic radar and sub-millimeter radiometer retrievals of ice hydrometeors in mid-latitude frontal cloud systems. Atmospheric Measurement Techniques, 2022, 15, 677-699.	3.1	5
123	Optically thin clouds in the trades. Atmospheric Chemistry and Physics, 2022, 22, 6879-6898.	4.9	5
124	Retrieval of upper tropospheric water vapor and upper tropospheric humidity from AMSU radiances. Atmospheric Chemistry and Physics, 2005, 5, 2019-2028.	4.9	4
125	Comparing upper tropospheric humidity from microwave satellite instruments and IGRA radiosonde data. , 2010, , .		4
126	Martian magnetism with orbiting sub-millimeter sensor: simulated retrieval system. Geoscientific Instrumentation, Methods and Data Systems, 2017, 6, 27-37.	1.6	4

#	Article	IF	CITATIONS
127	Inter-channel uniformity of a microwave sounder in space. Atmospheric Measurement Techniques, 2018, 11, 4005-4014.	3.1	4
128	A new climate data record of upper-tropospheric humidity from microwave observations. Scientific Data, 2020, 7, 218.	5.3	4
129	Emerging Technologies and Synergies for Airborne and Space-Based Measurements of Water Vapor Profiles. Space Sciences Series of ISSI, 2017, , 273-310.	0.0	4
130	Optimised frequency grids for infrared radiative transfer simulations in cloudy conditions. Journal of Quantitative Spectroscopy and Radiative Transfer, 2012, 113, 2124-2134.	2.3	3
131	Sub-millimeter observations of the terrestrial atmosphere during an Earth flyby of the MIRO sounder on the Rosetta spacecraft. Planetary and Space Science, 2013, 82-83, 99-112.	1.7	3
132	Modeling the Zeeman effect in high-altitude SSMIS channels for numerical weather prediction profiles: comparing a fast model and a line-by-line model. Atmospheric Measurement Techniques, 2016, 9, 841-857.	3.1	3
133	Onboard Radio Frequency Interference as the Origin of Inter-Satellite Biases for Microwave Humidity Sounders. Remote Sensing, 2019, 11, 866.	4.0	3
134	Characterization of the High-Resolution Infrared Radiation Sounder Using Lunar Observations. Remote Sensing, 2020, 12, 1488.	4.0	3
135	Lagrangian Coherent Structures and Vortex Formation in High Spatiotemporalâ€Resolution Satellite Winds of an Atmospheric Kármán Vortex Street. Journal of Geophysical Research D: Atmospheres, 2021, 126, e2021JD035000.	3.3	3
136	Are elevated moist layers a blind spot for hyperspectral infrared sounders? A model study. Atmospheric Measurement Techniques, 2021, 14, 7025-7044.	3.1	3
137	The COST 723 Action. Quarterly Journal of the Royal Meteorological Society, 2007, 133, 99-108.	2.7	2
138	Intercalibration of microwave temperature sounders using radio occultation measurements. Journal of Geophysical Research D: Atmospheres, 2015, 120, 3758-3773.	3.3	2
139	Calibration and Characterization of Satelliteâ€Borne Microwave Sounders With the Moon. Earth and Space Science, 2021, 8, e2021EA001725.	2.6	2
140	Comment on "Monitoring the atmospheric boundary layer by GPS radio occultation signals recorded in the open-loop mode―by S. Sokolovskiy et al Geophysical Research Letters, 2007, 34, .	4.0	1
141	Opportunistic Constant Target Matching—A New Method for Satellite Intercalibration. Earth and Space Science, 2020, 7, e2019EA000856.	2.6	1
142	CHAMP Radio Occultation Detection of the Planetary Boundary Layer Top. , 2006, , 265-272.		1
143	Toward a long-term homogenized UTH data set derived from satellite microwave measurements. , 2006, , ,		0
144	Correction to "Comparing upper tropospheric humidity data from microwave satellite instruments and tropical radiosondesâ€, Journal of Geophysical Research, 2011, 116, .	3.3	0

#	Article	IF	CITATIONS
145	The Representation of Tropospheric Water Vapor Over Low-Latitude Oceans in (Re-)analysis: Errors, Impacts, and the Ability to Exploit Current and Prospective Observations. Space Sciences Series of ISSI, 2017, , 227-251.	0.0	0
146	The In-Orbit Performance of SEVIRI From Observations of Mercury and Venus. IEEE Journal of Selected Topics in Applied Earth Observations and Remote Sensing, 2022, 15, 3215-3223.	4.9	0